Proceedings of ISFOG 2025
5TH INTERNATIONAL SYMPOSIUM ON
FRONTIERS IN OFFSHORE GEOTECHNICS
Nantes, France | June 9-13 2025

ISBN 978-2-85782-758-0

Effective Approaches in Seismic Design of Subsea Foundations

Hadi Suroor,[1*] Amir M. Kaynia[2] and Regis Wallerand[3]
[1]Energy Geotechnics, Katy, Texas, USA
[2]Norconsult AS, Sandvika, Norway
[3]TotalEnergies, Paris, France
[*]hadi@energy-geotechnics.com

ABSTRACT: In a gas development project offshore Africa, the subsea facilities are situated in a challenging geohazard-prone field, which includes seismicity-induced hazards. The presence of potentially liquefiable top sands posed significant design challenges for subsea facilities' foundation design. The conventional seismic design approach dictated a pile-supported foundation for all subsea structures to meet seismic stability and performance requirements, which would have resulted in schedule challenges, cost over-run, and risk of pile penetration in potently buried boulders. The geotechnical team adopted state-of-the-art seismic design approaches to alleviate these constraints and risks, which are often not used in subsea structure foundation design. First, a comprehensive cyclic laboratory testing program was developed to define the dynamic properties of siliceous carbonate sands and underlying clays due to the absence of publicly available reference data. Nonlinear site-response analyses used variable cyclic ground models to develop site-specific design response spectra. A methodology for estimating the damping of subsea foundations accounting for soil-structure interaction (SSI) was developed. The procedure was applied to a mudmat foundation supporting a PLET (Pipeline End Termination) structure, and the resulting SSI damping values for different directions were computed. The 5% damped response spectrum was modified using the SSI-damping in three directions. Finally, the performance of the subsea foundation was checked by performing a 2-dimensional finite-element-based dynamic analysis. These advanced seismic design approaches eliminated pin pile requirements for nearly 75% of the total subsea structures, offering considerable cost, schedule, and risk reduction.

Keywords: mudmat, seismic, damping, SSI, SRA

1 INTRODUCTION

In offshore Africa's gas development project, the subsea facilities are in a challenging geohazard-prone field. The presence of potentially liquefiable top sands posed significant design challenges for the design of subsea facilities' foundations. The conventional seismic design approach dictated a pile-supported foundation for all subsea structures to meet seismic stability and performance requirements, which would have resulted in schedule challenges, cost over-run, and risk of pile penetration in potently buried boulders. The geotechnical team adopted state-of-the-art seismic design approaches to alleviate these constraints and risks, which are often not used in subsea structure foundation design.

2 SEISMIC DESIGN APPROACH

Per the project requirements (standard in seismic design), the subsea systems shall be designed for two levels of seismic conditions, as defined below.

Strength Level Earthquake (SLE) has a return period of 200 years. Under this seismic event, the subsea systems will continue to operate normally, and no repairs are needed. Using the ISO terminology, the SLE event can be treated as Extreme Level Earthquake (ELE).

Ductility Level Earthquake (DLE) has a return period of 2000 years. Under this seismic event, major environmental damages must be avoided, and the integrity of the overall pipeline pressure must be maintained. However, major repairs may be needed. The DLE event can be treated as an Abnormal Level Earthquake (ALE).

At the onset of the detailed design, additional geotechnical and geophysical surveys were conducted to reduce the gap in the available data. An extensive cyclic laboratory testing program was carried out to develop site-specific dynamic soil parameters that are required for advanced seismic design, which consisted of the following evaluations and analyses: state-of-art liquefaction analysis to assess liquefaction potential, development of site-specific response spectra, assessment of structure-specific damping to reduce seismic loads, and dynamic near-field site response analysis to determine foundation performance during strong motions. These analyses achieved an optimized foundation design driven by seismic requirements. Some of these design approaches are briefly described below.

2.1 Development of Seismic Parameters

2.1.1 Seabed Stratigraphy

The soil stratigraphy within the deepwater manifold centers varies within the upper 10m with interbedded sand and clay layers. The thickness of the top sand layer ranges from about 0.4m to 10m, followed by overconsolidated high plasticity clays at up to 70m explored depths. Observation of numerous large boulders on the seabed led to suspect similar boulders in the sub-seabed; however, available surveys could not confirm it. The top sand layer comprises sand with silt, silty sands, and clayey sands with variable carbonate content. The relative density of sand layers varies from very loose to very dense but predominantly medium dense to dense.

The carbonate contents in the top sands range from about 50% to less than 90%; and can be classified as "calcareous" to "siliceous carbonate" according to the classification system by Clark and Walker (1977). The top sand layer was shown to be susceptible to liquefaction based on conventional CPT-based liquefaction assessment.

2.1.2 Shear Modulus and Damping Curves

Several resonant column tests were performed to develop site-specific Gmax, together with shear and damping relationships with shear strain. For the calcareous clays, it was observed that the curves proposed by Darendeli, 2001 fit the lab test results best.

However, the lab-derived relationship for calcareous sand samples deviates considerably from the published relationships for silica sands. The lab-based G/G_{max} and Damping Ratio (D) for silty sand (solid circles) derived from the resonant column and cyclic DSS tests are compared with the proposed correlation for siliceous carbonate soils presented in Flores et al., 2018 (solid lines), as can seen in Figure 1. There appears to be a little variation of G/G_{max} with shear strain with depths (shown from 0.1m to 8.95m) within the top sand layer.

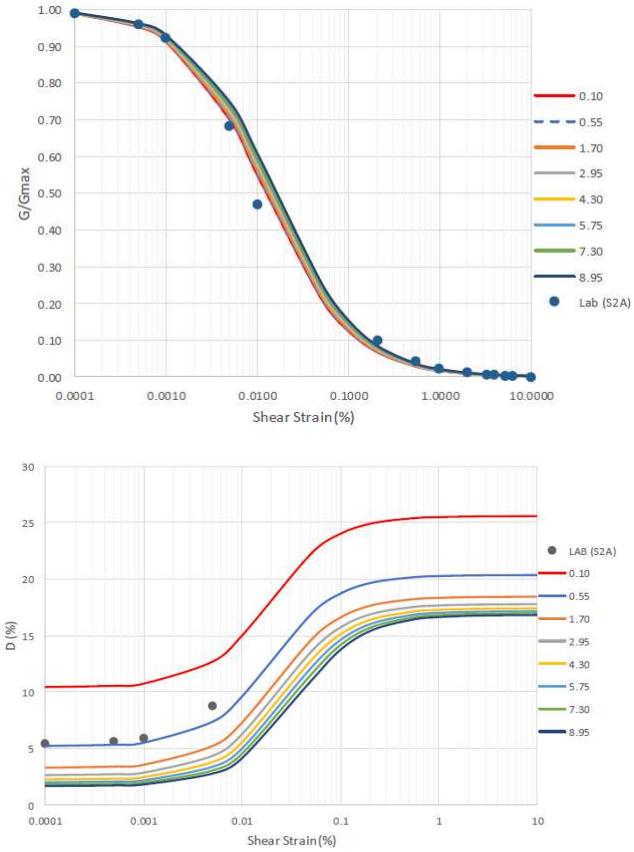

Figure 1. Shear modulus reduction and damping as a function of shear strain for sand layers

2.1.3 Cyclic Resistance Ratio

The cyclic DSS tests were performed on the intact soil samples collected from deepwater to evaluate the liquefaction potential of non-plastic (NP) soils (Table 2-1) . The cyclic resistance ratio (CRR) is defined as the cyclic shear stress (τ_{cy}) that causes liquefaction in the soil specimen divided by the applied effective vertical stress (σ_v') for a given number of load cycles. Liquefaction triggering is assumed to occur when the excess pore pressure ratio ($r_u = \delta u/\sigma_v'$) reaches 90% or cyclic shear strain (γ_{cy}) reaches 3%, whichever comes first.

Table 2-1 Recommended CRR for Deepwater

Sam-ple	Depth (m)	Type	FC (%)	CRR7.5
4A-3	8.33	Sand	10	0.207

2.2 Site-Specific Response Spectra

The site response analysis (SRA) has been performed to capture the nonlinear effect of potentially liquefiable sands overlying stiff soil. The merit of SRA to capture seabed non-linearity and evaluate

liquefaction triggering has been well demonstrated by Olson et al., 2019. The nonlinear-effective stress (NL-ES) site response analysis for the free-field (FF) condition was performed by the widely-used commercial software DEEPSOIL. The embedded soil models in DEEPSOIL have been calibrated using the project-specific geotechnical data. Two extreme soil profiles, one with 0.2m top sand (BH-01) and the other with 10m sand (BH-05), were analyzed for seven site-specific input ground motions. The profiles of average maximum excess pore pressure ratios and shear strains are shown in Figures 2 and 3, respectively. The effect of excess pore pressures and shear strain generated in the top sands are visible in the design response spectra compared to the uniform hazard spectra (see Figures 4 and 5).

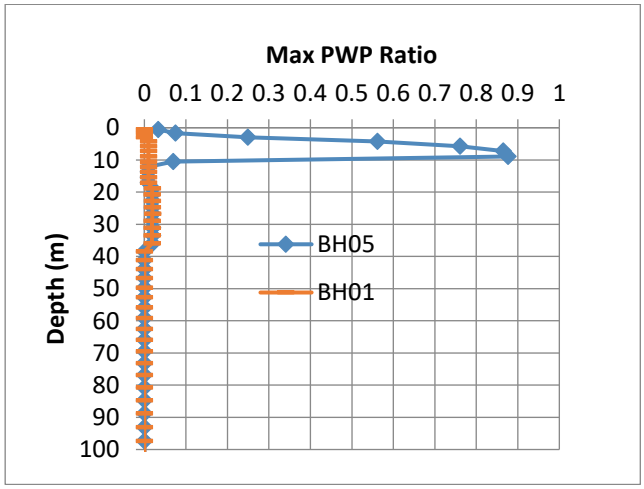

Figure 1 - Average Profiles of Maximum PWP Ratio for DLE motions.

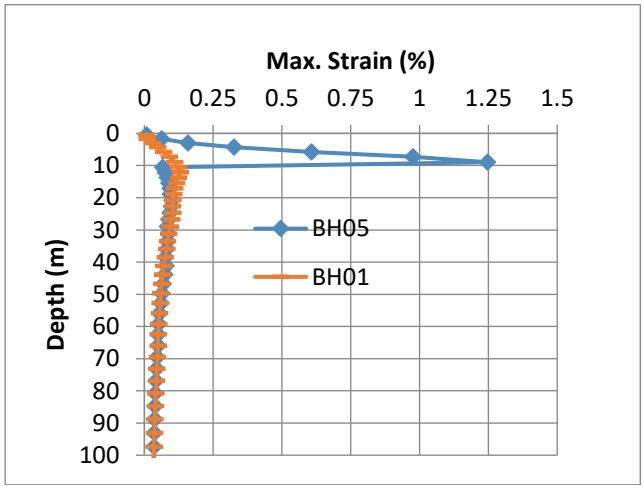

Figure 2 - Average Profiles of Peak Shear Strain for DLE motions.

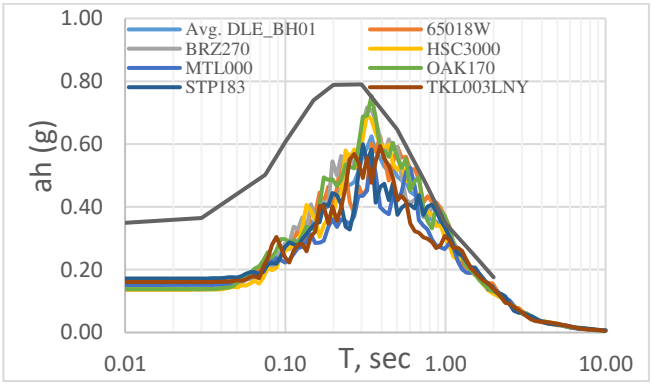

Figure 3 - 5% damped DLE Horizontal Response Spectra: BH-01.

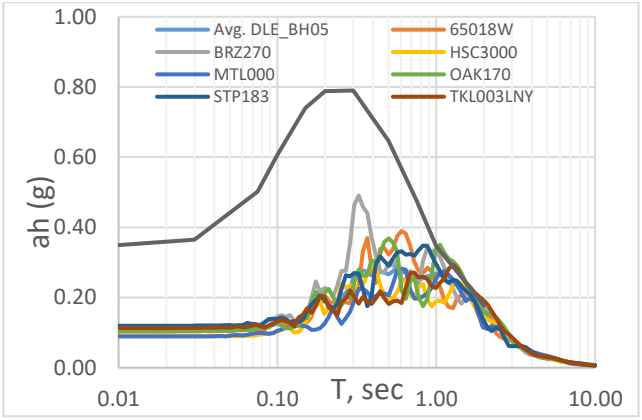

Figure 4 - 5% damped DLE Horizontal Response Spectra: BH-05.

2.3 SSI Damping

Most of the subsea structures were PLETs on 12m x 4m mudmats. From the estimated SSI natural frequency of these structures, it was evident that the damping of a mudmat-supported PLET (Figure 6) could be higher than the 5% assumed in developing the design spectra; therefore, the inclusion of SSI damping could reduce the seismic loads which were used for foundation response assessment.

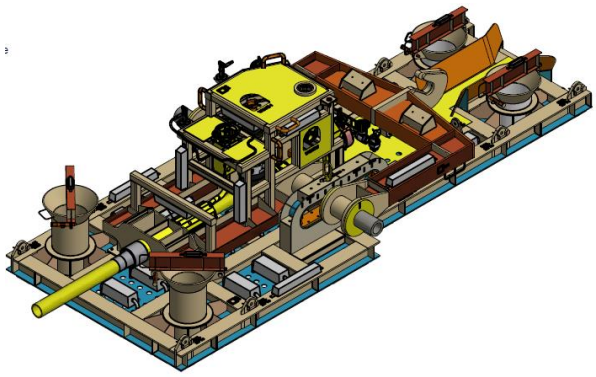

Figure 6. Isometric view of a PLET with mudmat

2.3.1 Computation of Model Parameters

To compute damping, one should first calculate the foundation impedance, the relationship between a harmonic (steady-state sinusoidal) force on the foundation, and the corresponding displacement. Such computations are often performed in the frequency domain, resulting in foundation impedances. Each impedance term is represented by a complex number, with the real part representing the combined effect of static stiffness and added soil mass and the imaginary part representing the damping. Damping includes hysteretic damping, which dominates at low frequencies, and radiation damping, which dominates at higher frequencies.

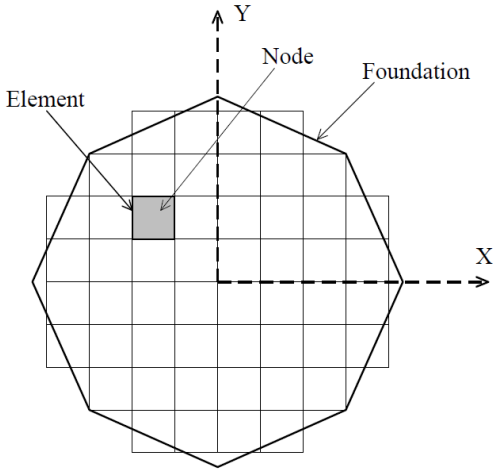

Figure 7 - Discretization of foundation-soil interface for computation of foundation impedance by Green's functions approach.

The solution used for the computations is based on the so-called Green's functions (e.g., Wong and Luco, 1976; Kaynia et al. 1997), which give the response in a domain for a unit load in any direction. The contact surface between the ground and the foundation is discretized into a regular grid of rectangular elements (Figure 7). By applying uniformly distributed unit loads on each element in the three directions and calculating the displacements at all element centers (nodes) using analytical Green's functions, one can derive the flexibility matrix of the ground/foundation interface, which can be inverted to compute the impedance matrix for the nodes expressed as:

$$\mathbf{P} = \mathbf{K}\,\mathbf{U} \qquad (1)$$

Where **P** is the vector of foundation-soil interface forces at the nodes, **U** is the vector of corresponding displacements, and **K** is a $3n \times 3n$ matrix where n is the number of nodes.

The calculations are carried out under steady-state harmonic loads at discrete frequencies ω. Note that the impedances represent stiffness/damping characteristics of the foundation; therefore, they are independent of the type of analysis, whether it is for external loading (like machine foundations) or earthquake loading. The impedances are used to extract discrete stiffness, add soil mass, and create a dashpot for foundations.

By applying the rigid foundation kinematics for each mode of vibration (3 translations and 3 rotations), one can compute the foundation's 6 × 6 impedance matrix (see Kaynia et al. 1997 for more details). The soil parameters needed for the analyses are the shear modulus, G, mass density, ρ, Poisson's ratio, ν, and hysteretic damping ratio, ξ, for each soil layer. For earthquake applications, the G and ξ are often selected as the values compatible with the effective earthquake-induced strains.

2.3.2 Foundation stiffness and damping ratio

The impedances of the foundation in the three translational directions and the three rotational directions as functions of frequency were computed using the numerical code described by Kaynia et al. (1997). The foundation damping ratio at a given frequency is calculated as $K_{imag}/(2*K_{st})$, where K_{imag} is the computed imaginary part of the impedance term at the considered frequency and K_{st} is the corresponding static stiffness. The values at low frequencies (here 0.5 Hz) indicate the hysteretic damping ratios. As frequency increases, the radiation damping dominates. Note that these are foundation damping only. The next section describes a procedure for estimating the global SSI damping. Figure 8 shows a plot of all damping ratios as a function of frequency.

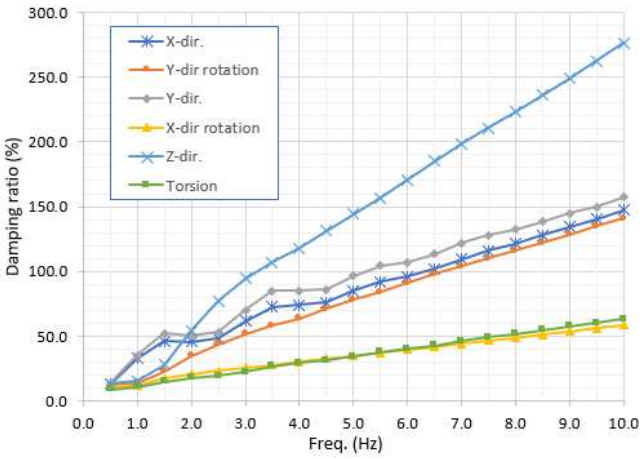

Figure 8 – Foundation damping ratios as functions of frequency for different directions of shaking

2.3.3 Equivalent damping accounting for SSI

Most structures, including subsea structures, are founded on foundations with hysteretic and radiation damping. For such foundation-structure systems, the classical mode shapes with real mode shapes do not exist, and one should use forced-vibration methods to estimate equivalent model damping.

This study developed a procedure to estimate the total damping (referred hereto as SSI damping). The procedure is inspired by the same principle used for an SDOF system excited by a harmonic load based on the concept of Dyn. Ampl. Factor (DAF). For a system with a mass M_0, stiffness K_0, and natural frequency ω_0, over a foundation with stiffness K_f, imaginary part of impedance, C_f, the DAF as a function of vibration frequency, ω, can be computed from:

$$DAF = \frac{1+i\frac{C_f}{K_0+K_f}}{\left[1-\left(\frac{\omega}{\omega_e}\right)^2\right]+i\frac{C_f}{K_f}\left[1-\left(\frac{\omega}{\omega_0}\right)^2\right]} \quad (1)$$

Where:

$\omega_0 = \sqrt{\frac{K_0}{M}}$ = natural frequency of structure on a rigid base.

$\omega_e = \sqrt{\frac{K_e}{M}}$ = (equivalent) natural frequency of SSI system, in which the equivalent SSI stiffness is given by $K_e = \frac{K_0 K_f}{K_0+K_f}$. Note that Eq. (1) can be used for both horizontal and vertical directions by using the applicable impedance terms K_f and C_f,

By equating the DAF from Formula (1) with that for an SDOF system as function of damping ratio, one can estimate the equivalent damping of the SSI system. Applying the above procedure to the results of the impedances for the vertical (Z-dir) and horizontal (X-dir) with natural periods 0.11 s. and 0.13 s., one can compute SSI damping equal to 30% and 22%, respectively. For a minimum damping of 22%, the seismic spectral acceleration is reduced by 50% compared to the 5% damped acceleration, which was adopted for seismic design (Table 2-2).

Table 2-2 Seismic Accelerations for Foundation Design

Seismic Event	Natural period (s)			5%/20% Damped Spectral Acceleration* (g)		
	X	Y	Z	X	Y	Z
SLE	0.13	0.20	0.11	0.16/0.08	0.20/0.10	0.10/0.05
DLE				0.24/0.12	0.32/0.16	0.16/0.08

Because the structure's response in the y-direction appears to be affected by rocking, an extended version of the model presented above is needed. Details of the rocking model is not presented herein due to space restriction.

However, despite the 50% reduction in seismic loading, the mudmat foundation failed to meet the seismic design requirements during the DLE, which led to the finite-element dynamic analysis of the mudmat foundation.

2.4 2D Response Analysis

In addition to the above assessments, a conventional code-based bearing capacity analysis of the mudmat was initially performed that accounted for the effect of excess pore pressures generated during earthquake shaking on the shear strength of the sand. However, the results showed unacceptable low factors of safety during the design DLE. As a result, two-dimensional (2D) nonlinear seismic response analyses (SRA) were performed in a finite element program using an advanced constitutive soil models and including mudmat. Some of the results of 2D-SRA are presented below. Details can be found in Carlton et al. (2023).

Figure 9 (a and b) shows the failure planes for the vertical bearing capacity analyses for the mudmat width (a) and the mudmat length models (b). The mudmat width model shows a double failure under both sides of the mudmat, whereas the mudmat length model predicts failure to the right, in the same direction as the applied horizontal load. The horizontal bearing capacity analyses (not shown) indicate a shallow sliding failure to the right. The predicted resistance in the horizontal direction is almost the same for both models. In contrast, the mudmat length model predicts a larger resistance in the vertical direction due to the larger size of the modeled mudmat. The 2D-SRA-derived foundation bearing capacity turned out to be considerably larger than simplified code-based bearing capacity, which resulted in satisfying the seismic performation requirements.

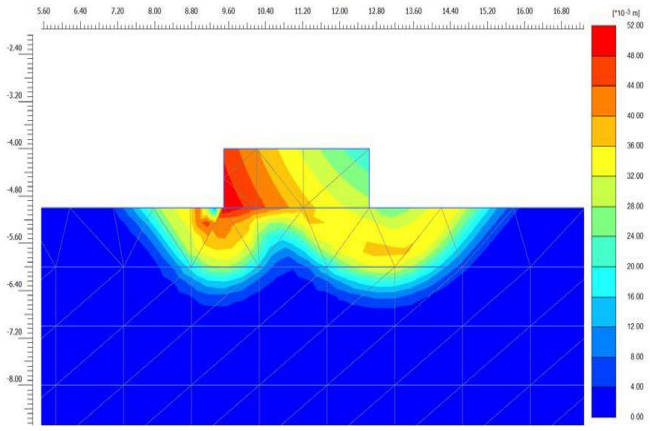

(a)

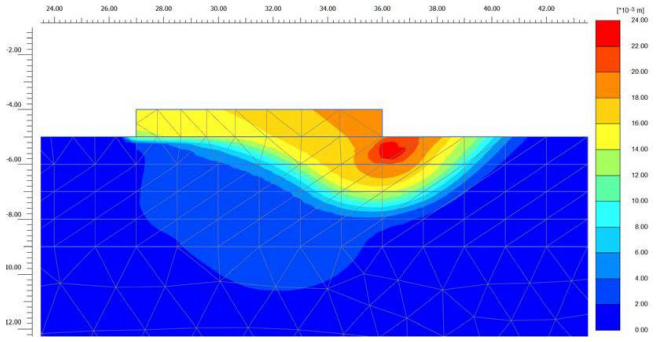

(b)

Figure 9 Failure plane for the vertical bearing capacity analysis for the mudmat width model (a) and mudmat length model (b)

3 OUTCOME

The design basis available at the beginning of the project indicated widespread liquefaction potential across the field based on the conventional CPT-based approach during both SLE and DLE seismic events. The seismic loading derived from the standard 5% damped spectra was too high for mudmat stability.

An advanced laboratory testing program was developed to develop site-specific dynamic soil parameters required for advanced analysis at the frontier development site. This program proved to be highly beneficial for the project in optimizing foundation design.

A new procedure was developed to derive SSI-induced damping for the subsea structures supported on mudmat. The higher SSI damping reduced the seismic loading by 50% compared to the 5% damping conventionally used in seismic loading calculation.

Finally, the 2D finite element-based site response analysis for the mudmat foundation validated satisfactory foundation performance and bearing capacities during DLE.

By adopting these advanced seismic design approaches, pin pile requirements were eliminated for nearly 75% of the total subsea structures, offering considerable cost, schedule, and risk reduction.

4 CONCLUSIONS

A systematic multifaceted seismic design approach for the subsea structure foundation, which was adopted in a frontier development project, has been presented in this paper. The conventional stability analysis combined with the beneficial SSI-induced damping effect could not meet the seismic foundation design requirements for the stronger ground motion. The state-of-the-art seismic foundation design approaches including 2D-SRA eliminated the need for pin piles for satisfying seismic foundation stability and performance, resulting in a considerable cost reduction, removal of schedule constraints, and reduction of installation risk.

AUTHOR CONTRIBUTION STATEMENT

H. Suroor: Data curation, Methodology, Analysis, Writing- Original draft. **A. Kaynia**.: Methodology, Analysis, Review. **R. Wallerand**: Reviewing, and Editing.

REFERENCES

Carlton, B., Suroor, H., Nadim, F. (2023). Seismic Stability Assessment of a Mudmat on Liquefiable Seabed. Proc. Offshore Technology Conference, Houston, TX.

Clark, A.R., Walker, B.F., 1977. A proposed scheme for the classification and nomenclature for use in the engineering description of Middle Eastern sedimentary rocks. Geotechnique 27, 93–99.

Darendeli, M.B. (2001). Development of a new family of normalized modulus reduction and material damping curves. Ph.D. dissertation, University of Texas, Austin, TX.

Flores Lopez, F.A. et al. (2018), Normalized modulus reduction and damping ratio curves for Bay of Campeche carbonate sands. Proceed. Offshore Technology Conference, Houston, TX.

Kaynia, A.M., Madshus, C., Furuhovde, R. and Jostad, H.P. (1997). Impedance Models for Machine Foundation Analyses. Proc. Conf. Ground Dyn. and Man-Made Processes, Inst. of Civil Engineers, London, UK, 173-183.

Olson, S. M., Mei X. And Hashash, Y. M. A. (2019). Nonlinear site response analysis with pore pressure generation for liquefaction triggering evaluation. Journal of Geotechnical and Geoenvironmental Engineering, ASCE.

Wong, H.L. and Luco, J.E. (1976). Dynamic response of rigid foundations of arbitrary shape, Earthquake Engng. Str. Dyn, 4, 579-587.